# Spin-polarized Auger electrons in core-valence-valence decays of 3*d* impurities in metals

M. I. Trioni,[1] A. Zanetti,[2] G. Fratesi,[1,2] and G. P. Brivio[1,2]
[1]*ETSF and CNISM, UdR Milano Bicocca, via Cozzi 53, I-20125 Milano, Italy*
[2]*Dipartimento di Scienza dei Materiali, Università di Milano-Bicocca, via Cozzi 53, I-20125 Milano, Italy*
(Received 26 January 2009; published 23 April 2009)

The spin polarization of the emitted electrons from 3*d* impurities in simple metal hosts in a core-valence-valence Auger process is analyzed in terms of a first-principles density-functional theory approach, by using the golden rule. The relationship between the spin-dependent local density of states, the magnetic moments of the 3*d* atoms and the energy-dependent and total spin polarization of the Auger electrons is discussed. It is shown how to estimate the magnetic moment of the impurities from a measure of the total spin polarization of the Auger electrons. This can be achieved considering (i) that the Auger signal is simply due to the impurities only, (ii) the very locality of the Auger phenomenon, and (iii) a simple and general relationship between the spin polarization and the magnetic moment of the impurity which we show to be independent of the metal host.

DOI: 10.1103/PhysRevB.79.165115 PACS number(s): 71.15.Mb, 76.30.Fc, 82.80.Pv, 32.80.Hd

## I. INTRODUCTION

The core-valence-valence (CVV) Auger electron spectroscopy has shown itself capable of detecting spin-polarized electrons. The first experiment was performed on a ferromagnetic glass.[1] In this case the spin polarization of the Auger electron was ascribed to the Fe atoms. Later it was demonstrated that a spin asymmetry of the Auger electron may not only be derived from that of a magnetic sample, but also by the polarization properties of the incident primary electron or by the helicity of the impinging light radiation, which creates the initial core hole.[2,3] Theoretical results extend from the self-consistent studies of the Auger spin-polarized electrons from a K surface[4] to the relativistic Korringa-Kohn-Rostoker calculations of Auger spin-polarized spectra, within a density-functional theory (DFT) approach and including spin-orbit coupling, performed for paramagnetic Pd and ferromagnetic Fe,[5] to studies by the Hubbard model.[6]

For several alloy systems with 3*d* impurities, the emitted electrons could be spin polarized, and indeed polarized Boron electrons have been detected by spin-resolved photoemission in Co-B and Fe-B alloys.[7] Auger spectroscopy is a widespread method also to analyze such systems. However, in most of Auger spectroscopy experiments this technique is not exploited to measure spin polarization of the secondary electrons, but only to probe the composition and the structure of the sample during growth with no spin resolution. For example, see the very recent studies of ferromagnetic alloy films of transition metals.[8,9] For quasicrystals such as Al-rich alloys with low concentration of Mn impurities, diamagnetism, paramagnetism, ferromagnetism and spin-glass behavior have been reported for different AlMn phases.[10,11] These investigations have been coupled to DFT calculations of the interaction energies among 3*d* or 4*d* impurities in Al-rich alloys.[12] Recent DFT studies carried out for 3*d* and 4*d* impurities in transition metals[13] and Si,[14] emphasize the interest for such systems.

Since theoretical investigations within a first-principles framework on spin-polarized Auger electrons from metal alloys seem lacking, to our knowledge, in this work we wish to present a systematic theoretical study of the Auger core-valence-valence spectra of 3*d* impurities in simple enough metals. Our approach is based on the golden rule expression for the transition rate, the DFT framework, and the Green's function embedding approach for computing the electronic properties of the system.[15] The substrate is described by jellium. This simple model is able to capture general trends in several systems. For the systems under investigation we believe that this model does not oversimplify the substrate for Al and Mg, while its lack of *d* electrons should not affect the main qualitative trends of the results for noble metal hosts. We find that 3*d* impurities in simple and noble metals eject Auger electrons which are spin polarized. The relationship between the impurity magnetic moment and total spin polarization of the Auger electrons is worked out and the result is independent of the substrate.

The paper is organized as follows. In Sec. II we shall outline the theory, in Sec. III we shall present the model system, while Sec. IV deals with the calculated Auger spectra. Finally, Sec. V will be devoted to conclusions.

## II. THEORY

In order to calculate the CVV Auger spectrum from magnetic impurities diluted in metal hosts, we make use of the two step model which neglects the coupling between the creation of the initial core hole and the successive Auger de-excitation, and it is valid for a long living core hole.[16] We concentrate on the second step of the process, i.e., the decay of a valence electron on the core state and the emission of the Auger electron. We use the Fermi golden rule to write down the transition probabilities and assume that the initial state consists of one core hole in the Fermi sea and the final one of two valence holes plus the unbounded Auger electron.

If one takes into account the spin degrees of freedom, it is possible to consider four different elementary processes displayed in Fig. 1. On the left of the vertical dashed line all the electronic states, the core, the Auger, and the valence majority ones exhibit spin up, while on the right all states have spin down, the valence ones referring to the minority population. The black balls represent initially empty electronic states, while the white ones initially occupied states. The

 

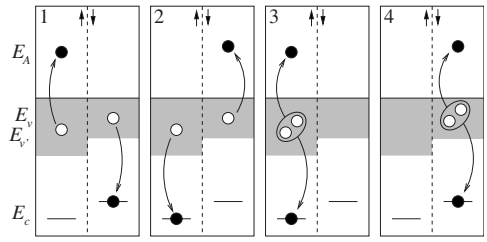


FIG. 1. Different processes contributing to the Auger rate.

process 1 (and 3) differs from 2 (and 4) only via a spin-flip of all the electrons involved in the de-excitation. Consequently for nonmagnetic systems processes 1 and 2 are completely equivalent as well as processes 3 and 4. On the other hand, for magnetic systems, processes 1 and 2 probe the two spin populations in a different way, while processes 3 and 4 involve only one spin component, the majority and the minority one for process 3 and 4, respectively.

Looking at processes 1 and 2, one observes that the spins of the two valence electrons involved in the de-excitation are antiparallel. They are instead parallel in processes 3 and 4. Due to the Pauli exclusion principle one expects that the probability density to find two electrons with parallel spin near the nucleus of the impurity will be lower than that for two electrons with antiparallel spin. Consequently, processes 3 and 4 will give smaller contributions to the Auger rate than 1 and 2.

For the present treatment, we neglect the interaction between the two valence holes in the final state. This is a good approximation for systems with delocalized valence states. Hole-hole interaction effects, such as multiplet structures in the Auger spectra, are relevant to the line shape for narrower bands, including some of the cases discussed in the following. For closed shell systems the on-site interaction can be treated within a two particle Dyson's equation Green's function formalism[17,18] and has been recently implemented in an *ab initio* scheme.[19] However, in such an approach the proper evaluation of matrix elements, which is crucial to the present work, is so far replaced by atomic results. By using an independent-particle approximation some of the spectra shown in the following will describe experimental results only qualitatively. However, we expect energy-integrated quantities such as the total Auger rate to be well represented.

In order to calculate the transition probabilities $\mathcal{P}_{\sigma_c}(E_{a\sigma_a})$ from the core state of energy $E_c$ and spin $\sigma_c$ to the Auger electron state of energy $E_a$ and spin $\sigma_a$, we follow the approach introduced in Ref. 20 and later developed for metastable de-excitation spectroscopy (MDS) within the embedding framework.[21] In short we assume that an electron with spin $\sigma$ is removed from the impurity core level and write down the Auger CVV transition rates by using the golden rule. We distinguish between transitions with opposite and same spins for the core and Auger electron:

$$\mathcal{P}_{\sigma}(E_{a\bar{\sigma}}) = 4\pi \sum_{v,v'} \int d\hat{k}_a |M_{a\bar{\sigma},c\sigma,v\sigma,v'\bar{\sigma}}|^2 \times \delta(E_{a\bar{\sigma}} + E_{c\sigma} - E_{v\sigma} - E_{v'\bar{\sigma}}), \quad (1)$$

$$\mathcal{P}_{\sigma}(E_{a\sigma}) = 2\pi \sum_{v,v'} \int d\hat{k}_a |M_{a\sigma,c\sigma,v\sigma,v'\sigma} - M_{a\sigma,c\sigma,v'\sigma,v\sigma}|^2 \times \delta(E_{a\sigma} + E_{c\sigma} - E_{v\sigma} - E_{v'\sigma}), \quad (2)$$

where $\bar{\sigma}=-\sigma$, $E_{a\sigma}=k_a^2/2$ is the energy of the Auger electron, and $E_{v\sigma}$ that of a valence electron of spin $\sigma$. In Eqs. (1) and (2), reported in Hartree atomic units, the Coulomb matrix elements are given by

$$M_{A,C,V,V'} = \int d\mathbf{r}_1 d\mathbf{r}_2 \frac{\psi_V(\mathbf{r}_1)\psi_C^*(\mathbf{r}_1)\psi_{V'}(\mathbf{r}_2)\psi_A^*(\mathbf{r}_2)}{|\mathbf{r}_1 - \mathbf{r}_2|}. \quad (3)$$

In Eq. (3), $\psi_A$ describes the wave function of the Auger electron, $\psi_C$ the orbital of the initial core hole, and $\psi_V$ and $\psi_{V'}$ are the final valence state hole wave functions, all of them containing their spin vector. Such wave functions are evaluated within the DFT by solving the Kohn-Sham (KS) equation in the local spin-density approximation. They are worked out applying the final state rule in which the system is described in its ground state.[22] The initial and final states are taken as single Slater determinants.

The Auger processes involving two electrons with opposite spins, processes 1 and 2 in Fig. 1, are described by the matrix element in Eq. (1). They normally dominate with respect to processes 3 and 4, which instead refer to parallel valence spins. Their rates are defined by Eq. (2) which contains an interference term due to the antisymmetric configurational part of the wave function.

## III. MAGNETIC IMPURITIES IN SIMPLE METALS: MODEL SYSTEM

We solve the KS equation for a single impurity in infinite jellium which is characterized by the proper valence charge density $\rho=\frac{3}{4\pi r_s^3}$ of the real system. We make use of the Green's function embedding approach[23,24] and we perform an all-electron calculation upon expansion on a linearized augmented plane waves (LAPW) basis set.[25]

The removal of a substrate atom is obtained by creating a spherical vacancy of radius $r_{\mathrm{ws}}=\sqrt[3]{Z_{\mathrm{val}}}r_s$ ($Z_{\mathrm{val}}$ being the number of the host valence electrons) in the positive jellium background. The KS equations are solved in a spherical region of radius equal to 7 $a_0$ ($a_0$ being the Bohr radius), which contains essentially all the perturbation induced by the atomic impurity. All computational parameters (kinetic energy cutoff, number of spherical waves, etc.) have been verified to give fully convergent results.

In order to present a wide phenomenology of the magnetic behaviors, we choose the magnetic $3d$ impurities hosted by different simple and noble metals. Explicitly, we consider V, Cr, Mn, Fe, and Co impurities in Al, Mg, Cu, and Ag hosts, whose relevant parameters are reported in Table I. For the purposes of the present paper, it is relevant to look at the density of states (DOS) in the impurity atomic region. In Fig. 2 some results spanning the most representative systems are reported. Observe the smooth structure of the majority and minority DOS calculated in a sphere of radius 3 $a_0$ around the impurity. The DOS's computed in denser elec-

TABLE I. Main parameters used to describe the metal hosts.

| Host | Ag | Mg | Cu | Al |
|---|---|---|---|---|
| $r_s(a_0)$ | 3.02 | 2.66 | 2.67 | 2.07 |
| $Z_{\text{val}}$ | 1 | 2 | 1 | 3 |
| $r_{\text{ws}}(a_0)$ | 3.02 | 3.35 | 2.67 | 2.98 |
| Bandwidth (eV) | 5.49 | 7.08 | 7.03 | 11.69 |

tronic substrates such as Al are broader while the peaks of the majority and minority spin contributions get closer. Moreover, the relevance of the exchange contribution is reflected in the separation of the peaks. While the $d$ band, neglected by jellium, influences the properties of noble metal hosts, nevertheless the impurity resonances do not overlap the energy region of such band in most cases. This warrants the use of such a simple model for the aims of this paper.

In Table II we display our calculated magnetic moments, $\mu_{\text{loc}}$, of the selected systems starting from the Ag substrate, in which the $3d$ impurities present the largest $\mu_{\text{loc}}$ due to the relatively small electron density of the metal host, up to the densest Al substrate. Note a few systems with no spin asymmetry. The magnetic moments are reported in units of Bohr magnetons $\mu_B$ and are worked out within the Wigner Seitz sphere $V_{\text{ws}}$ of radius $r_{\text{ws}}$, using the following equation:

$$\mu_{\text{loc}} = \int_{V_{\text{ws}}} d_3\mathbf{r} \int_{-\infty}^{E_F} dE[\rho^{\uparrow}(\mathbf{r},E) - \rho^{\downarrow}(\mathbf{r},E)], \tag{4}$$

being $\rho^{\sigma}(\mathbf{r},E)$ the local DOS per spin $\sigma$, and $E_F$ the Fermi level. Comparisons with previously reported values of $\mu_{\text{loc}}$ are overall very good.[26]

## IV. SPIN-DEPENDENT AUGER SPECTRA

We will consider the $M_1VV$ transition in which the initial core hole is in the $3s$ level. This transition is easier to treat than those involving core states with higher angular momentum but still allows one to study the effect of the magnetization of the impurity on the Auger spectrum. Also it presents a larger exchange splitting in the core state than that of the lower-$s$ core ones ($K_1$ and $L_1$).

We discuss now the calculated $M_1VV$ Auger spectra for each process reported in Fig. 1 for V, Cr, Mn, Fe, and Co, whose DOS's are plotted in Fig. 2. Results are shown in Fig. 3. We point out that, once the spin direction of the electron removed from the core is fixed, the spin-resolved Auger spectrum shows a strong asymmetry, both for magnetic and nonmagnetic systems. The latter one is, for example, Co in Al, which we examine first. Indeed, as previously pointed out, $\mathcal{P}_{\sigma}(E_{a\bar{\sigma}})$ (processes 1 and 2) is much larger than $\mathcal{P}_{\sigma}(E_{a\sigma})$ (processes 3 and 4), whose squared matrix elements are reduced by interference, as already pointed out. This effect is larger for narrower bands, eventually leading to a null rate in the limiting case of sharp atomic states. Since the system is nonmagnetic, the Auger rates for processes 1 and 2 are identical, as well as those for processes 3 and 4. Before discussing the Auger rate for magnetic systems, we would like to mention that the line shape for $\mathcal{P}_{\sigma}(E_{a\bar{\sigma}})$ may be described by the convolution of the DOS integrated in suitable volumes, following a common approach due first to Lander,[27–29] but that of $\mathcal{P}_{\sigma}(E_{a\sigma})$ requires a full calculation of the matrix elements as in the present work.

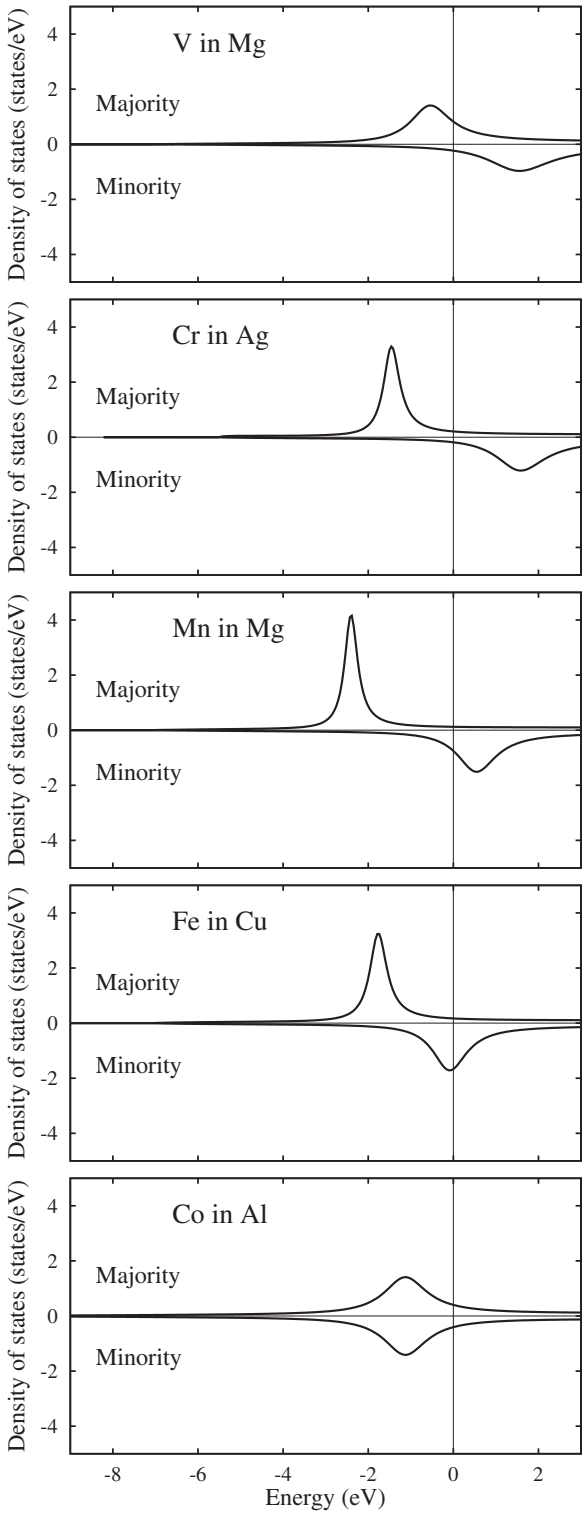


FIG. 2. Density of states of selected $3d$ impurities in different metals calculated in a sphere of radius 3 $a_0$. The energy reference is the Fermi level.

TABLE II. Local magnetic moments for various impurities in different metal hosts in units of the Bohr magneton.

| Impurity | Ag | Mg | Cu | Al |
|---|---|---|---|---|
| V | 3.22 | 3.02 | 2.44 | 0.00 |
| Cr | 4.23 | 4.12 | 3.48 | 1.95 |
| Mn | 4.06 | 3.96 | 3.31 | 2.27 |
| Fe | 2.85 | 2.75 | 2.19 | 1.19 |
| Co | 1.39 | 1.24 | 0.00 | 0.00 |

For magnetic systems, the transition rates are no longer symmetric with respect to a spin-flip of the core and Auger electrons. In particular, we consider Cr in Ag, which is the most magnetic of the investigated systems. Similar observations will hold for other cases, though to a reduced extent. A few considerations follow from the inspection of Fig. 3. First, the rates for processes 1 and 2 are different, the latter getting smaller than the former. This is due to the different matrix elements, $|M_{a\uparrow,c\downarrow,v\downarrow,v'\uparrow}|^2$ for process 1 and $|M_{a\downarrow,c\uparrow,v\uparrow,v'\downarrow}|^2$ for process 2. Second, process 4 is nearly suppressed, since it involves two electrons belonging to the minority spin population, while the opposite occurs for process 3 which two majority spin electrons participate to. Finally, only for this specific case, process 3 is enhanced as much as to become comparable to process 2. It is noteworthy that the interference effects tend to suppress the transition rate of processes 3 and 4 only for an initial *s* core level, while they solely reduce the contributions of such processes if the core hole is created in a *p* shell (not shown here).

In order to compare the calculated rates $\mathcal{P}_\sigma(E_{a\sigma'})$ with the measured spectra, the former must incorporate a broadening due to the hole-lifetime and to experimental resolution; in particular $M_1$ core holes undergo Coster-Kronig $M_1$-$M_{2,3}X$ transitions that lead to natural widths of 2 eV order.[30] This broadening will affect the line shape of a measured spectrum in an obvious way, while it does not modify any quantity which is energy integrated (such as the total spin polarization, defined later). From the experimental point of view, once the macroscopic magnetization of the sample is fixed, we can ionize the core level in two ways (or combinations of the two): by removing the core state electrons either selecting its spin or not. The former result can be achieved by a suitable probe, for example a photon with fixed helicity. A coincidence measurement between the photoelectron and the Auger electron could provide the same evidence. The latter result can be achieved by an impinging electron beam which is not selective to the spin of the core electrons. Consequently in Fig. 3 the curves represent for each impurity the spin-resolved contributions to the Auger spectrum. According to the experiment, suitable combinations of such four basic rates will be measured.[31] If the same population of spin-up and spin-down core holes is created by the probe, it is necessary to sum up the decays due to the various processes contributing to the Auger electrons of the same spin.

In other words the two spin signals are given by summing the rates (reported in Fig. 3) 1 plus 3 and 2 plus 4, respectively. This determines the de-excitation rate, for a fixed spin of the Auger electron, shown in Fig. 4 and defined as

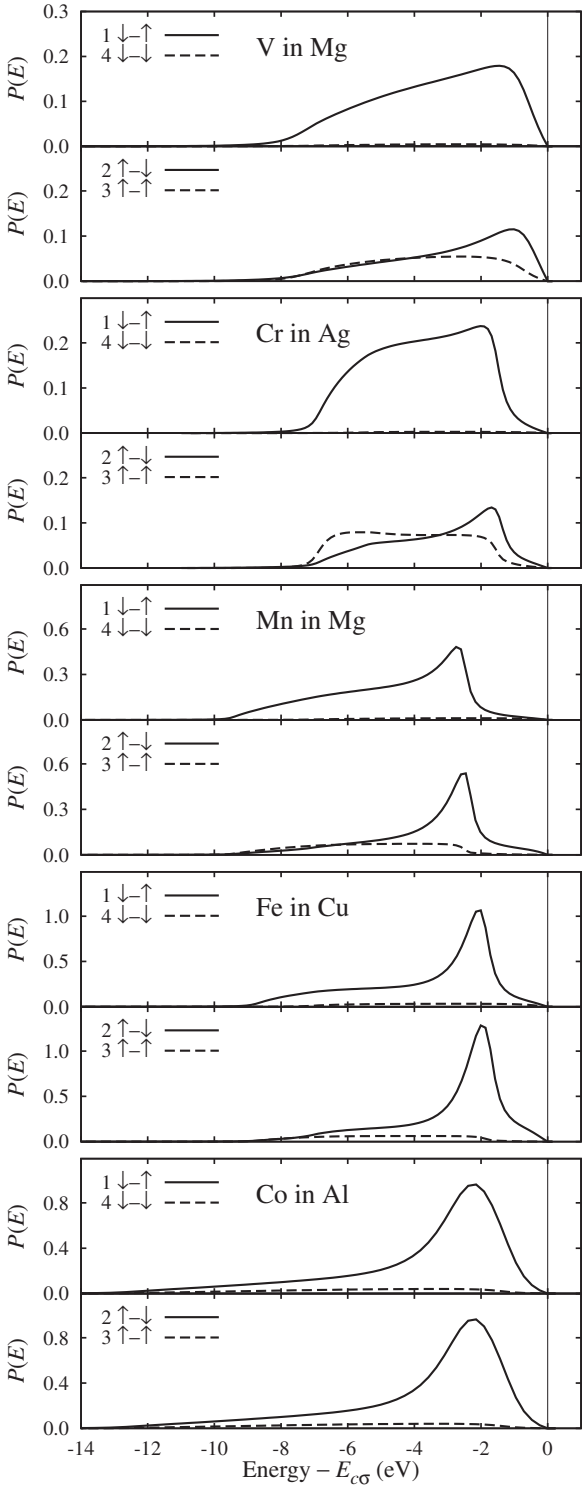


FIG. 3. CVV Auger transition rates for each process reported in Fig. 1. The energy is given with reference to that of the core state. For details see the text.

$$\mathcal{P}(E_{a\sigma}) = \mathcal{P}_\sigma(E_{a\sigma}) + \mathcal{P}_{\bar{\sigma}}(E_{a\sigma}). \tag{5}$$

Note that to plot the rate as function of the emitted electron energy, one must take into account two different spin-dependent energies of the 3*s* core states in the energy conservation in Eqs. (1) and (2). So the core level energy

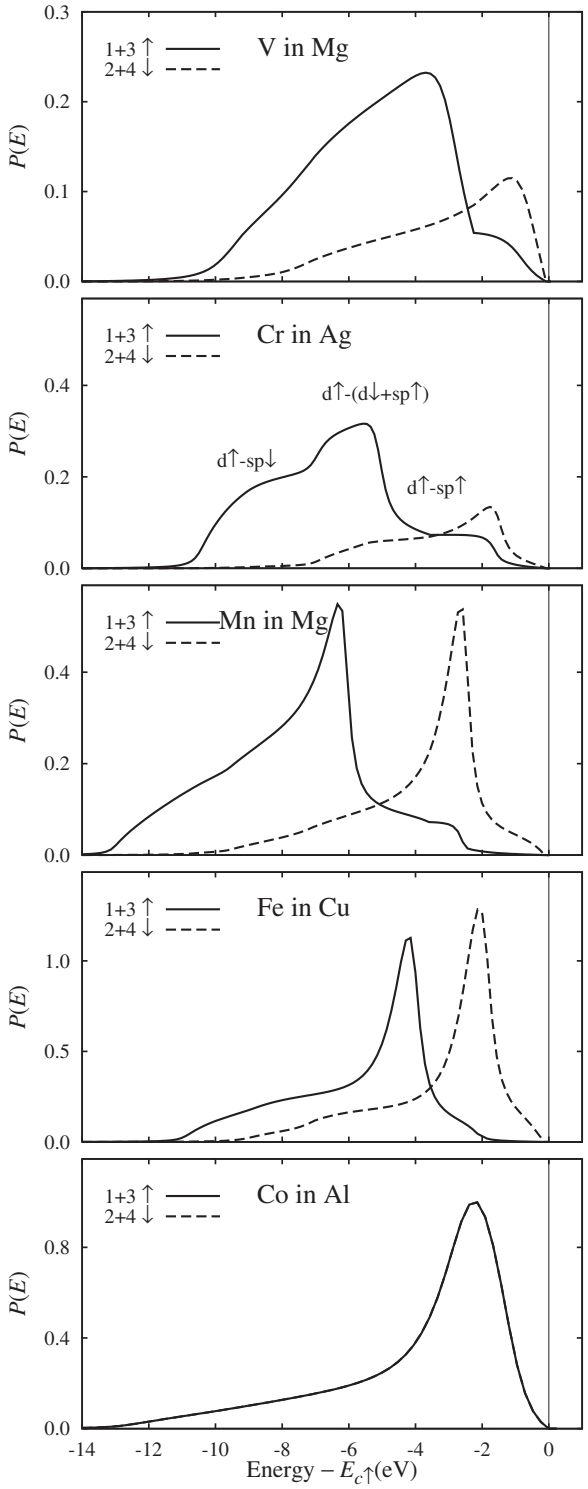


FIG. 4. Auger rate, $\mathcal{P}(E_{a\sigma})$, for both majority (solid line) and minority (dashed line) spins. The energy is given with reference to that of the majority spin core state.

spitting will be found in the Auger electrons.

For a nearly closed valence shell system (Co in Al), hence with no magnetic moment, the two line shapes for $\mathcal{P}(E_{a\uparrow})$ and $\mathcal{P}(E_{a\downarrow})$ superimpose. As the system gets more and more magnetic, the difference between the Auger spectra for the two spin components becomes more and more evident starting from Fe in Cu. In this case the main feature is the energy splitting of the main Auger peak, but moving upward in Fig. 4 both the intensity and the line shape differ more significantly. As previously pointed out the most magnetic of the investigated systems is represented by Cr in Ag. In this case the line shape of the Auger spectrum is more structured and in Fig. 4 the valence states contributing to the spin-up peaks are also reported.

TABLE III. Spin polarization [see Eq. (7)] of the Auger electrons for various impurities and metal hosts (in percentage).

| Impurity | Ag | Mg | Cu | Al |
|---|---|---|---|---|
| V | 52.8 | 43.8 | 34.5 | 0.0 |
| Cr | 54.4 | 47.5 | 36.9 | 13.8 |
| Mn | 29.4 | 26.4 | 19.2 | 9.0 |
| Fe | 3.7 | 2.6 | 3.4 | 0.8 |
| Co | −1.4 | −1.8 | 0.0 | 0.0 |

In order to quantify the amount of total spin polarization of the Auger spectra, we use the following quantity, $I^{\sigma}$,[4] evaluated by integrating the spin-polarized rates:

$$I^{\sigma} = \int dE_{a\sigma} \mathcal{P}(E_{a\sigma}), \tag{6}$$

over the energy of the emitted electron and define the spin polarization by

$$\mathcal{S} = \frac{I^{\uparrow} - I^{\downarrow}}{I^{\uparrow} + I^{\downarrow}}. \tag{7}$$

This quantity (in percentage) is reported in Table III for all systems considered in Table II.

Indeed it can be very large. For example see that for V and Cr impurities in metal host of lower density. On the other hand, the small magnitude of the polarization for Fe and Co suggests that a measurement of such a quantity might not be sensitive enough to detect any spin asymmetry.

A quantitative comparison of the results of the impurity magnetic moment in Table II with those of the total spin polarization presented in Table III shows that there is no intuitive way to relate them. But if we take into account the rescaled quantity with respect to the number of impurity $d$ valence electrons, i.e., $\mu_{\mathrm{loc}}/N_d$, we can work out a meaningful relationship between the magnetic moment and the spin polarization of the Auger spectrum of different atoms in each substrate. Such a dependence is reported in Fig. 5. Here we can appreciate a general trend for transitions involving $s$ core states for all substrates (this generality is of great relevance since it suggests that this correlation is independent of the chosen host and further justifies *a posteriori* the use of a simple jellium model for the substrate), i.e., $\mu_{\mathrm{loc}}/N_d$ being proportional to the square root of the polarization:

$$\frac{\mu_{\mathrm{loc}}}{N_d} \approx 1.45\sqrt{\mathcal{S}}. \tag{8}$$

Here the functional dependence has been chosen for simplicity. A direct proportionality between $\mu_{\mathrm{loc}}/N_d$ and $\mathcal{S}$ may be

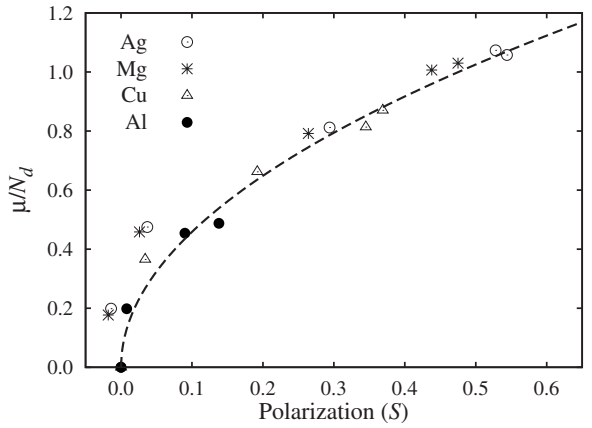


FIG. 5. Correlation between the spin polarization of the Auger electrons and the magnetic moment. The dashed line is the expression given in Eq. (8).

expected using the Lander approach,[27] namely, that the Auger rates are given by the convolution of the DOS's. The effect of process 3 which becomes more relevant for magnetic systems acts to deviate the relationship between $\mu_{\mathrm{loc}}/N_d$ and $\mathcal{S}$ from a linear behavior and can be suitably fitted by Eq. (8). Hence we can provide an estimate of the impurity magnetic moment from a measurement of the polarization of the Auger signal by taking its square root and multiplying it times the number of impurity $d$ electrons. The error on the rescaled magnetic moment is smaller than 0.05 $\mu_B$ in all cases where the polarization is relevant.

## V. DISCUSSION AND CONCLUSIONS

In this paper we studied the spin-polarized CVV Auger spectra from 3*d* impurities diluted in simple metal hosts. The electronic properties of these systems have been worked out in the DFT framework and the two particle wave functions have been built using a single Slater determinant of KS orbitals. The golden rule has been applied to calculate the transition rates, also taking into account the spin degrees of freedom. This generalization has allowed us to correctly consider the interference term, as in previous works about the deexcitation of metastable helium (MDS),[21,32] which can play a significant role in determining the Auger spectrum.

First we analyzed the spin dependence of the Auger spectra for nonmagnetic systems, for a removed core electron of fixed spin.[33] Second, for magnetic 3*d* impurities diluted in metals, we have calculated the spin-resolved Auger spectra, either for spin selective core ionization or not.

The structure of the Auger line shapes can be affected by the simple jellium model adopted for the substrate, and by the single particle approach, which does not include the interaction between the two valence holes. Conversely, the energy integrated quantities such as the polarization of the emitted Auger electrons are more reliable. The main contribution of this paper is the suggestion of a simple relationship between such a polarization and the magnetic moment of the impurity which is fairly well satisfied by our systems and it is independent of the metal host.

Because of the very locality of the Auger process with respect to other photoemission techniques, one can access the valence electronic and magnetic properties of very diluted impurities. In this context, a very important goal is to measure the magnetic moment of the impurities. To this end our results suggest the following procedure. By looking at the kinetic energy spectrum corresponding to a specific Auger transition, one selects univocally the atomic species. Next, by measuring the polarization of the Auger electrons one should be able to get a good estimate of the magnetic moment using the proposed relationship between these two quantities.

In order to compare our results with experiments one must be aware of the assumption that the sample is globally magnetized, i.e., with majority spin components aligned. In metals this could be hardly obtained, especially for diluted alloys where the macroscopic magnetic field may be negligible. On the other hand, the anisotropy on the metal surfaces is able to align the magnetic moments of atomic impurities and thin adlayers and this suggests one to consider these systems in the experimental investigations. The more promising technique in detecting the spin polarization of the Auger electrons is the Auger photoelectron coincidence spectroscopy.[34] In fact it looks to be extremely surface sensitive, it is able to strongly reduce the signal from the secondary electrons, and it can correlate the photoelectron with the Auger electron via their spins, angles, and energies.[35]

[1] M. Landolt and D. Mauri, Phys. Rev. Lett. **49**, 1783 (1982).
[2] R. Allenspach, D. Mauri, M. Taborelli, and M. Landolt, Phys. Rev. B **35**, 4801 (1987).
[3] A. Chassé, H. A. Dürr, G. van der Laan, Y. Kucherenko, and A. N. Yaresko, Phys. Rev. B **68**, 214402 (2003).
[4] Y. Kucherenko and P. Rennert, Phys. Rev. B **58**, 4173 (1998).
[5] J. Minár, V. Popescu, and H. Ebert, Phys. Rev. B **62**, 10051 (2000).
[6] T. Wegner, M. Potthoff, and W. Nolting, Phys. Rev. B **61**, 1386 (2000).
[7] Y. B. Xu, D. Greig, E. A. Seddom, S. Cornelius, and J. A. D. Matthew, IEEE Trans. Magn. **35**, 3427 (1999).
[8] H. Y. Ho, Y. S. Lin, E. J. Huang, Y. J. Chen, and C. S. Shern, Surf. Sci. **601**, 615 (2007).
[9] K. J. Kim, D. W. Moon, C. J. Park, D. Simons, G. Gillen, H. Jin, and H. J. Kang, Surf. Interface Anal. **39**, 665 (2007).
[10] V. Simonet, F. Hippert, M. Audier, and G. Trambly de Laissardière, Phys. Rev. B **58**, R8865 (1998).
[11] D. Nguyen-Mahn and G. Trambly de Laissardière, J. Magn. Magn. Mater. **262**, 496 (2003).
[12] T. Hoshino, N. Fujima, M. Asato, and R. Tamura, J. Alloys Compd. **434-435**, 572 (2007).
[13] S. N. Mishra, Phys. Rev. B **77**, 224402 (2008).
[14] Z. Z. Zhang, B. Partoens, K. Chang, and F. M. Peeters, Phys.

Rev. B **77**, 155201 (2008).
[15] N. Bonini, M. I. Trioni, and G. P. Brivio, Phys. Rev. B **64**, 035424 (2001).
[16] O. Gunnarsson and K. Schönhammer, Phys. Rev. B **22**, 3710 (1980).
[17] M. Cini, Solid State Commun. **20**, 605 (1976).
[18] G. A. Sawatzky, Phys. Rev. Lett. **39**, 504 (1977).
[19] G. Fratesi, M. I. Trioni, G. P. Brivio, S. Ugenti, E. Perfetto, and M. Cini, Phys. Rev. B **78**, 205111 (2008).
[20] P. J. Feibelman, E. J. McGuire, and K. C. Pandey, Phys. Rev. B **15**, 2202 (1977).
[21] N. Bonini, G. P. Brivio, and M. I. Trioni, Phys. Rev. B **68**, 035408 (2003).
[22] D. E. Ramaker, Phys. Rev. B **25**, 7341 (1982).
[23] J. E. Inglesfield, J. Phys. C **14**, 3795 (1981).
[24] M. I. Trioni, G. P. Brivio, S. Crampin, and J. E. Inglesfield, Phys. Rev. B **53**, 8052 (1996).
[25] M. I. Trioni, S. Marcotulio, G. Santoro, V. Bortolani, G. Palumbo, and G. P. Brivio, Phys. Rev. B **58**, 11043 (1998).
[26] R. M. Nieminen and M. Puska, J. Phys. F: Met. Phys. **10**, L123 (1980).
[27] J. J. Lander, Phys. Rev. **91**, 1382 (1953).
[28] P. Weightman, M. Davies, and J. E. Inglesfield, Phys. Rev. B **34**, 6843 (1986).
[29] M. I. Trioni, G. Butti, and N. Bonini, J. Phys.: Condens. Matter **16**, S2923 (2004).
[30] M. Ohno and G. A. van Riessen, J. Electron Spectrosc. Relat. Phenom. **128**, 1 (2003) and references therein.
[31] R. Gotter, F. Da Pieve, A. Ruocco, F. Offi, G. Stefani, and R. A. Bartynski, Phys. Rev. B **72**, 235409 (2005).
[32] M. Alducin, R. Díez Muiño, and J. I. Juaristi, Phys. Rev. A **70**, 012901 (2004).
[33] It is worth noting that also the spectra summed over the core electron spins differ from those calculated via a spin-independent treatment, as used, for example, in Ref. 15.
[34] G. Stefani, R. Gotter, A. Ruocco, F. Offi, F. Da Pieve, S. Iacobucci, A. Morgante, A. Verdini, A. Liscio, H. Yao and R. A. Bartynski, J. Electron Spectrosc. Relat. Phenom. **141**, 149 (2004).
[35] R. Gotter, F. Offi, F. Da Pieve, A. Ruocco, G. Stefani, S. Ugenti, M. I. Trioni, and R. A. Bartynski, J. Electron Spectrosc. Relat. Phenom. **161**, 128 (2007).